Радиофизика и радиоастрономия, 1997, т. 2, №4, стр. 402-418

JOVIAN DECAMETRIC EMISSION: Regular Variabilities and Scale Invariants in S-Burst Dynamic Spectra

Boris P. Ryabov[1], Philippe Zarka[2], Helmut O. Rucker[3], Vladimir B. Ryabov[1], Mohammed Y. Boudjada[3]

[1] *Institute of Radio Astronomy, Ukrainian National Academy of Sciences, 4 Chervonopraporna st., Kharkiv, 310002, Ukraine*

[2] *Observatoire de Paris-Meudon, F-92195 Meudon Cedex, France*

[3] *Space Research Institute, Halbärthgasse 1, 8010 Graz, Austria*

The paper is received by editor December, 12, 1997

An unique combination of the large decameter array UTR-2 with recently installed high resolution acousto-optical spectrograph (AOS) and super fast multichannel spectrograph (MCS) has resulted in a lot of fine structured, highest sensitivity dynamic spectra of S-bursts in the 10-30 MHz continuous frequency range. The majority of S-bursts shows a negative frequency drift, however separate parts of many complicated ones have a positive drift. Most of S-burst spectra are very complicated, while the relatively simple, linear in the f-t plane, spectra are in evident minority. The set of 56 types schematic images of individual S-bursts observed during observational campaigns in 1994-1996 is given. Some complicated spectral images of S-bursts demonstrate features of apparent self-similarity in different frequency-time scales. Other self-similar shapes appear repeatedly, from 2 to 10 times during 3 s period and occur in the records of different years. The long series of S-bursts are concentrated within slow drifting (~1.4 kHz/s) spectral sub-bands, whose central frequencies are separated by about 3.5 MHz.

On the basis of the observations performed we propose an operation algorithm of S-emission source and scheme of large-scale dynamics for the Io's tube radiating interval. The detected spectral features are consistent with the recently proposed model of S-burst generation, where the bursts are associated with ruptures of elemental current filaments around IFT on its surface.

1. Introduction

Since the fundamental discovery of sporadic DAM emission from Jupiter [1] the number of observations has reached many hundreds and the interest is continuously increasing to the radio planet.

Sporadic radiation from Jupiter is observed from about 100 kHz to 39.5 MHz and is caused by broadband noise storms mainly of two types, named L and S. At the output of the narrow-band receiver the L-emission appears as a post detector noise voltage with a time scale from 1 to 10 s, and S-emission is a series of short pulses with pulse duration from about 1 to 10 ms.

The fine structure of dynamic spectra of the S-component from Jupiter's radio emission has been studied for about forty years [2-25]. High frequency-time (f-t) resolution has been achieved in some observations, but many of them lack either high sensitivity or sufficiently long duration of tracking time (minutes) compared to the average duration of the S-burst storms (hours).

Before the observations were made with the UTR-2 radio telescope in Kharkiv [26-32] large-scale characteristics of the dynamic spectra of S-burst storms in a wide frequency range (more then 15 MHz) with long tracking duration and minimum flux about 10 Jy have not been sufficiently studied. Our recent observations of S-burst storms provide a possibility to study in details both spatial and frequency structure of the S-emission radiation pattern and to draw information about the geometric structure of the Io Flux Tube (IFT) and its dynamics.

The theory of Jupiter decametric radiation is still far from completeness. The paper [33] contains the full comparative survey of many earlier ones. The latest theoretical models of Jupiter S-burst emission generation mechanism are proposed in [34-36]. We will not consider here their advantages and deficiencies, and expound below the our physical model of the S-burst radiation source.

On the basis of accumulated observational data, a physical model of the radiation source and the mechanism responsible for the S-component [28,31,32] has been proposed. The model is consistent with angular parameters of the emission cone [30,46], planet's magnetic field structure [38-40], estimated location of the source [27,29], observed fine structures in S-burst spectra, frequency drift rates [12,13, 15-17,21], and other characteristics of emission.

Since 1991, a fruitful cooperation has been established between the Institute of Radio Astronomy, Ukrainian National Academy of Sciences and Space Research Institute, Austrian Academy of Sciences, devoted to the study of Jovian decametric (DAM) emission with very high f-t resolution [41]. In 1993 the French team from the Paris-Meudon Astrophysical Observatory joined this research. So far, five observational campaigns of Jupiter on the radio telescope UTR-2 with both French acousto-optical spectrograph and Austrian multichannel digital hardware have been carried out.

The unique combination of the world largest decameter array UTR-2 with recently installed high resolution acousto-optical spectrographs (AOS) and multichannel spectrograph (MCS) containing 30 receivers with super fast data acquisition cards allowed to obtain many high sensitivity spectral records of S-bursts in the frequency range from 10 to 30 MHz of sources Io-B, Io-C, and Io-A/C [37,42-44].

The UTR-2 decameter radio telescope [45] located near Kharkiv has the array surface about 150 thousands sq m, the updated continuous operating band about 8-30 MHz, tracking ability for all the sky hemishere, and multi-beam phasing system of the telescope allowing to perform the "on-off" observational regime. The minimal flux density detectable by the telescope is a function of frequency, changing from 100 to 10 Jy in the range 10÷25 MHz. The AOS that has been used simultaneously with very fast (2 ms) multichannel analyzer, provides a frequency-time resolution (12 kHz – 5 ms) in the total frequency band of 26 MHz.

Raw data of S-burst dynamic spectra have been processed by the specially designed software to remove long time scale interferencies, perform adaptive frequency-time interpolaton of S-burst spectra, and create the optimal amplitude transformation of the signals recorded. The software permits to restore the fine time-frequency structures in the dynamic spectra and thus to improve the finite resolution of the observational data. The time resolution in AOS data is increased by the cost of redundant frequency resolution, and frequency resolution of multichannel spectrum analyser for the cost of its high time resolution. The data processing also gives the possibility to distinguish the weak parts of S-bursts signals from unavoidable man-made interferencies.

2. Atlas of Jovian S-Burst Spectra and Phenomenology

High quality records made in 1994-1996 years are included to the new Atlas of Jovian Millisecond Radio Bursts (to be published soon). In contrast with earlier Atlases of Jovian S-bursts [12,15,21] we report mainly about high sensitivity, wide band, and long tracking time observations of S-burst storms which exhibit complex S-burst spectral patterns.

Most of the recorded in this period S-burst spectra reveal complicated spectral patterns, while relatively simple, quasilinear in f-t plane, spectra are in evident minority. As a rule, the spectra show a negative frequency drift with time. However, certain parts of many complicated burst patterns have the positive one. Usually, during an S-burst storm observed at the Earth, three stages of complexity in the amplitude-frequency-time space can be distinguished, and each stage lasts for several tens of minutes. At the initial stage, quasilinear negatively drifting bursts of moderate amplitude and lifetime about 50 ms intersecting the frequency band of 2÷4 MHz are observed. This corresponds to the traditionally expected, simplest patterns of Jovian S-radiation (Fig. 1). The middle stage is characterized by an enhanced amplitude, and increased complexity of individual patterns as is shown in Fig. 2. At the end of an S-burst storm, the situation resembles the initial stage. It should be however noted that zooming in time, frequency, and/or amplitude of bursts may reveal complicated intrinsic details or structures in the dynamic spectra, like those shown in Fig. 3. But so well organized spectral patterns do not always occur at the final stage, and dynamic spectra may also look noisy or random (Fig. 4).

Consider now the simplest, quasi linearly drifting S-bursts. After zooming in time, they look like symbol $\int$ in the f-t plane. An example of such behavior is given in Fig. 5, where the record of July 24, 1994 made with MCS is plotted at the time resolution of 2 ms. The end parts of $\int$-bursts are characterized by short duration at a fixed frequency (about 2 ms), comparatively slow drift rate and small flux density. In the middle of an $\int$, i. e. near the central burst frequency, the fixed-frequency duration increases up to 15 ms, as well as the drift rate and flux density. The total frequency bandwidths of individual S-bursts ranges from about 1÷2 MHz up to 6.5 MHz.

Another feature of S-burst storms is the concentration of S-burst sequences within well separated frequency bands (Fig. 6). An interesting property of S-emission is temporal variation of the width of bands over the time scale of several minutes. During the evolution of an S-burst storm, the change of the frequency width of bands from 1 to 6 MHz is observed. In Fig. 6,a one can see two such bands: the narrow one (about 1 MHz) with central frequency about 24 MHz, and the wide band one (4 MHz) occupying the lower part of the spectrum. Forteen minutes later, up to three frequency subbands, near 16, 20 and 24 MHz, coexist in the f-t plane (Fig. 6,b). It should be noted that in Fig. 6,b the opposite situation occurs, in the sense that the narrow band emission occupies lower frequencies, ~16 MHz, and wideband S-bursts appear at higher ones.

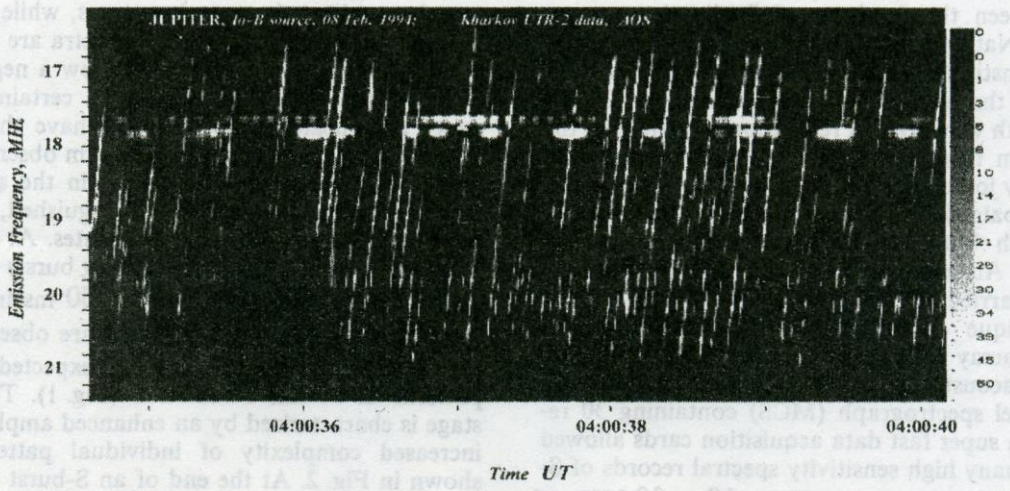

Fig. 1. *Simple, linearly drifting dynamic spectra of S-bursts that correspond to the initial stage of Io tube excitation when the magnetic field topology is not strongly distorted yet*

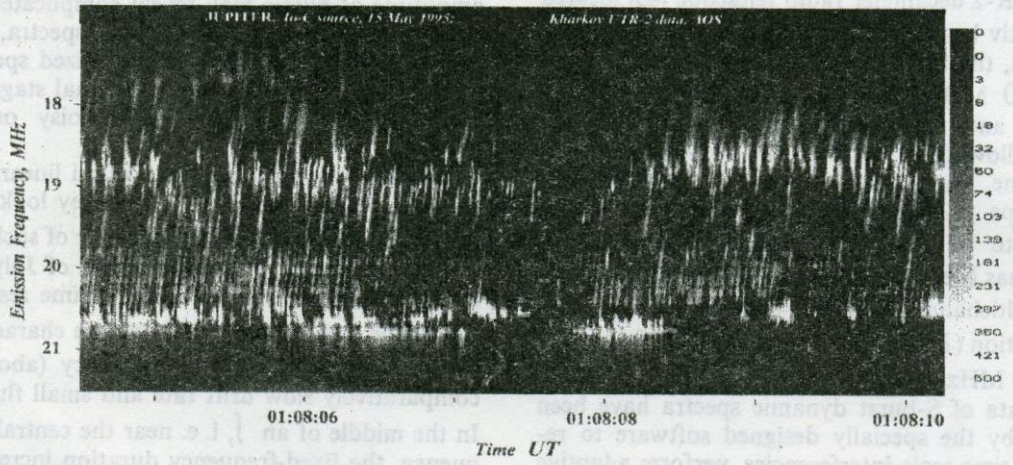

Fig. 2. *Some complicated S-burst spectra observed when the local magnetic field structure in the DAM emission zone of the Io tube is drastically disturbed*

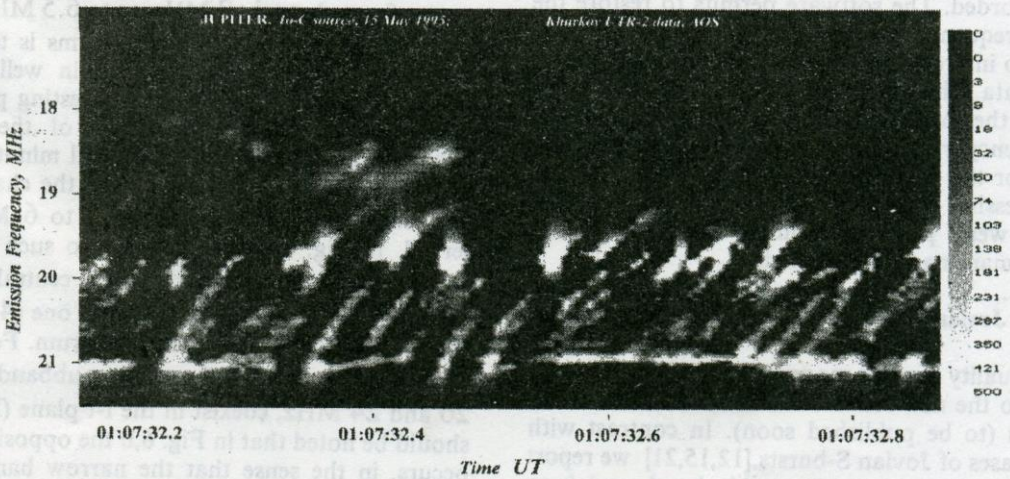

Fig. 3. *Some zoomed, complicated, well organized S-burst spectra with repetitive images of individual bursts*

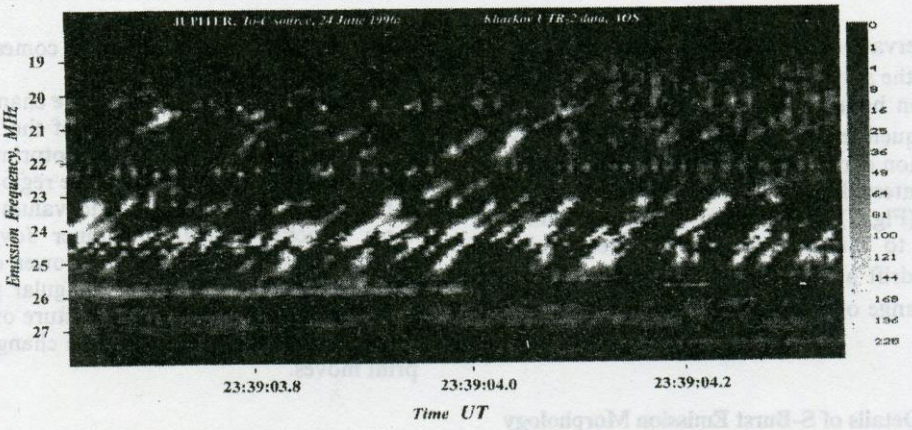

Fig. 4. *Random-like, dotted images of spectra which take place when electrical current circuits and field topology in S-burst radiating place of the Io tube is extremely disturbed*

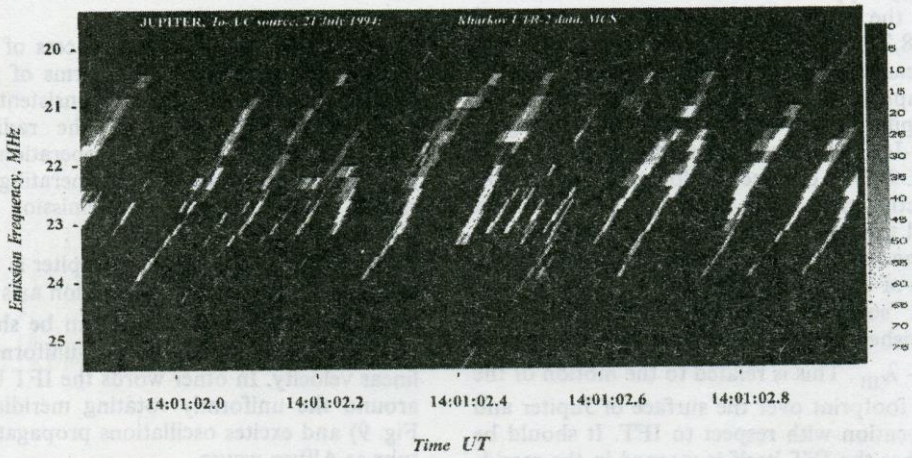

Fig. 5. *Zoomed, quasilinear images of S-bursts spectra of changing thickness and drift rate over the f-t plane*

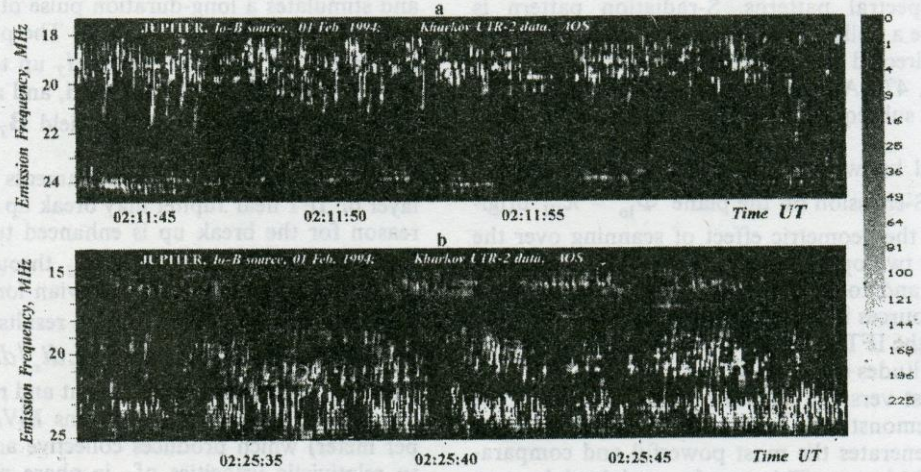

Fig. 6. *The S-burst sequences located on the frequency-time plane within well separated frequency subbands: a) two bands, b) three frequency subbands, near 16, 20 and 24 MHz. In Fig. 6,a the narrow bandwidth (about 1 MHz) of bursts occurs at upper frequency 24 MHz, but wideband (~4 MHz) S-bursts occupies the lower side of the spectrum. The opposite situation is shown at Fig. 6,b, where the narrow band emission (~1 MHz) occurred at lower frequency 16 MHz, and wideband (~3MHz) S-bursts moved to upper frequencies*

Our observations reveal also a new peculiarity of S-emission: the slow positive frequency drift $(df/dt)_{sb}$ of S-emission bands. Usually, the bands are located near the frequencies of 13, 16.5, 20, 23.5, 27 MHz and S-emission occurrence probability calculated over long time intervals [26] possesses maxima at those frequencies (Fig. 7). However, at time scales from tens of seconds to minutes, the central frequencies of bands may drift at an average rate about 1.4 kHz/s through a range of ± 1.5 MHz around the mean values.

3. Some Details of S-Burst Emission Morphology

It is largely supposed that the S-emission source is located in the upward stream branch of IFT [2-4,7,8,13,18,27]. The electric current system of IFT is a nonlinear distributed structure which demonstrates complicated spatiotemporal dynamics. A sketch of Jupiter-Io current circuit is shown in Fig. 8. The Jupiter-Io geometry underlying S-emission is given in Fig. 9. One can see the location of emission cones and active intervals in the IFT. Their evolution in space and time at timescales of tens of minutes is defined by the Jupiter-Io electric current, the topology and strength of local magnetic field.

So-called "sources" of Jovian S-emission are usually distinguished according to their position on the plane $\Phi_{Io} - \lambda_{III}$. This is related to the motion of the Io flux tube footprint over the surface of Jupiter and observer's location with respect to IFT. It should be also noted that the IFT itself is warped in the meridian plane that leads to additional complexity of the observed spectral patterns. S-radiation pattern is known to be a hollow cone, with large apex angle and cone axis directed along the IFT at the point of generation [46, 47]. All these aspects will be taken into account for subsequent interpretation of S-burst spectra.

The well known way of representing the distinct sources of S-emission on the plane $\Phi_{Io} - \lambda_{III}$ originates from the geometric effect of scanning over the observer by two opposite sides of the hollow emission cone (Io-B and Io-C). Another cause of the presence of several sources is the variation in the activity of the Io tube, as the IFT footprint passes by different active Jovian longitudes (Io-A, Io-D).

The most versatile shapes of the S-burst f-t patterns are demonstrated by the Io-C source, while the Io-B one generates the most powerful and comparatively simple bursts. This can be explained by two main reasons. The first one is different geometry of the radiation source in the IFT with respect to an observer. The Io-C source corresponds to the configuration when the observer looks to the concave side of the tube, whereas Io-B radiation comes to the Earth from the convex side of IFT.

The second reason is due to the change of physical conditions with local longitude of the IFT footprint on the surface of Jupiter. The footprint trajectory in the polar area of Jupiter lies in the regions with different magnetic field strength and values of the transverse velocity through the inner Jovian magnetosphere. As a consequence, the power of S-emission, frequency band, polarization, angular parameters of the radiation cone, and fine structure of spectral patterns on dynamic S-burst spectra change as the footprint moves.

4. Operation Algorithm of the S-Burst Emission Source

An interpretation of the process of S-bursts generation can be performed in terms of self-organized critical phenomena which is consistent with the recently developed model of the radiation source [28,31,32]. The scheme of the operation algorithm of the Jupiter-Io current system generating S-emission is shown in Fig. 10, and IFT S-emission zones are depicted in Fig. 11.

As the magnetic dipole of Jupiter is 10 degs tilted with respect to the planet's rotation axis and is shifted from its center by $0.1R_J$, it can be shown that the IFT footprint evolves with non-uniform angular and linear velocity. In other words the IFT base oscillates around the uniformly rotating meridian of Io (see Fig. 9) and excites oscillations propagating along the tube as Alfven waves.

An Alfven wave arising near Jupiter moves to Io and stimulates a long-duration pulse of integral electro-motive force (e. m. f.) on Io. The pulse results in an increase of the tube current i_T up to 10^8 A [48], growth in the local magnetic field, and appearance of the strong azimuthal magnetic field $\mathbf{B}_T$ produced by the current (see Fig. 11).

Elementary helical current filaments in the surface layer of IFT near Jupiter may break up abruptly. The reason for the break up is enhanced tube current i_T and tube transverse velocity $\mathbf{v}_S$ through the inner magnetosphere at two active Jovian longitudes: near 220 and 40 degs. The break up results in a pulse of the self-induction e. m. f. $u_x = L di_x/dt$ between the edges of disrupted helical filament and rise of an electric field of local strength of tens MV/m (Megavolt per meter) which produces collective acceleration up to relativistic velocities of in-phase radiating electrons (bunches). The velocity vector $\mathbf{v}_e$ of a bunch is directed along the helical magnetic field:

$$\mathbf{B}_S = \mathbf{B}_J + \mathbf{B}_T$$

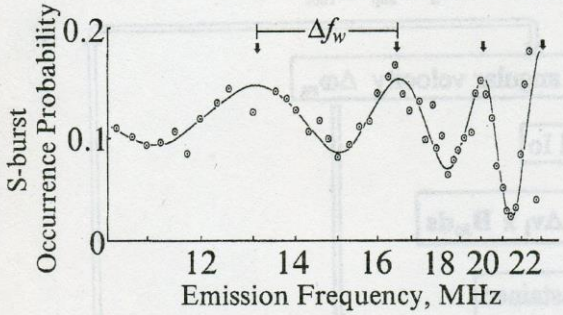

Fig. 7. *The S-burst occurrence probability vs emission frequency calculated over the long time interval [26]*

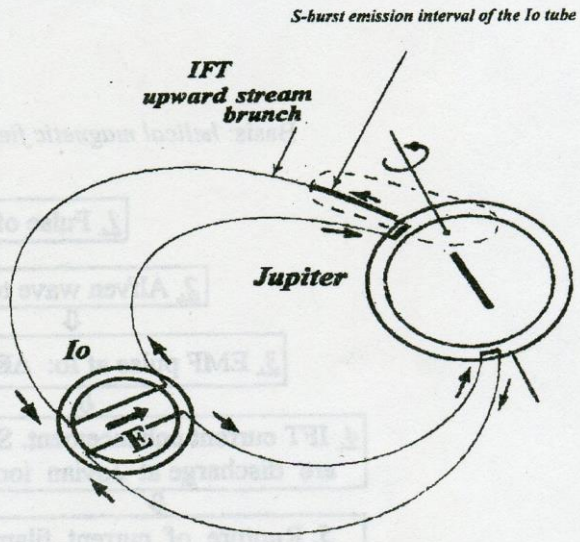

Fig. 8. *Sketch of the Jupiter-Io current circuit*

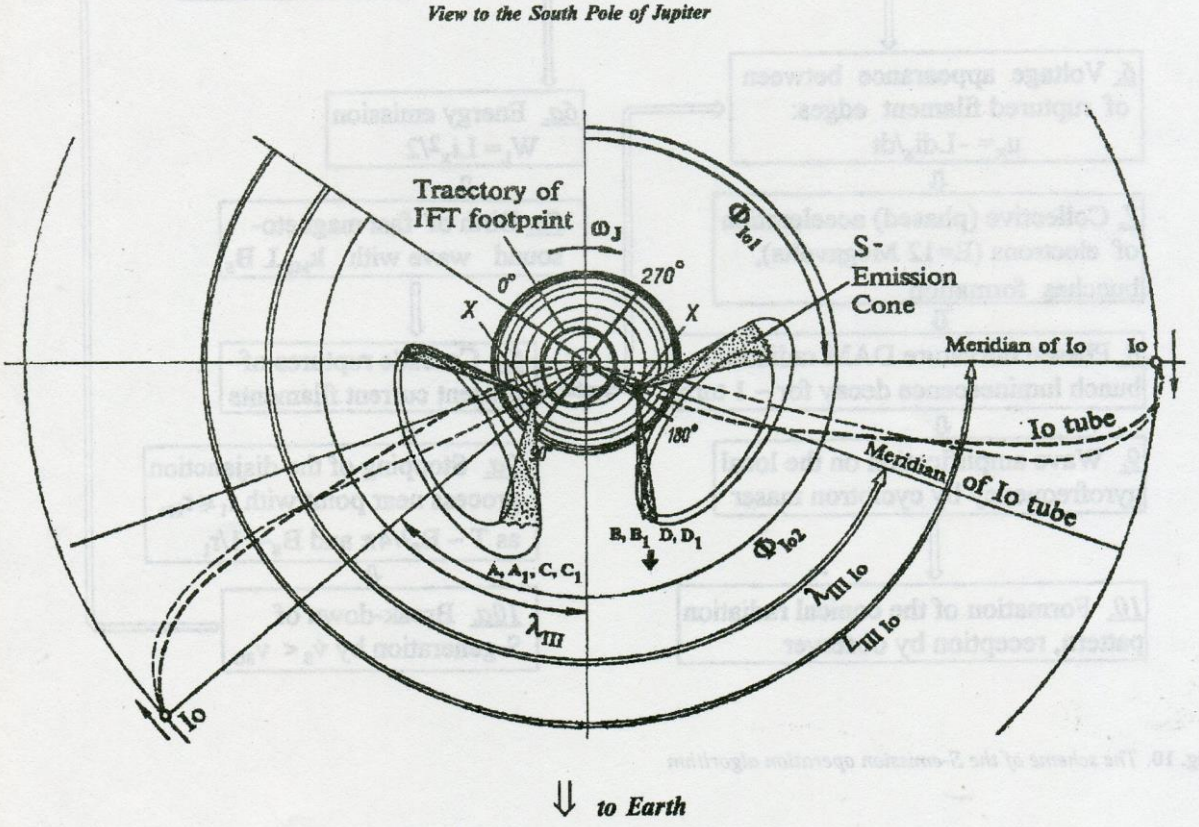

Fig. 9. *The Jupiter-Io geometry in connection with the S-radiation: location of the emission cones and DAM-active intervals of the Io tube. Their space-time evolution in the scale of tens of minutes is defined by Jupiter-Io electric current and local magnetic field strength and topology*

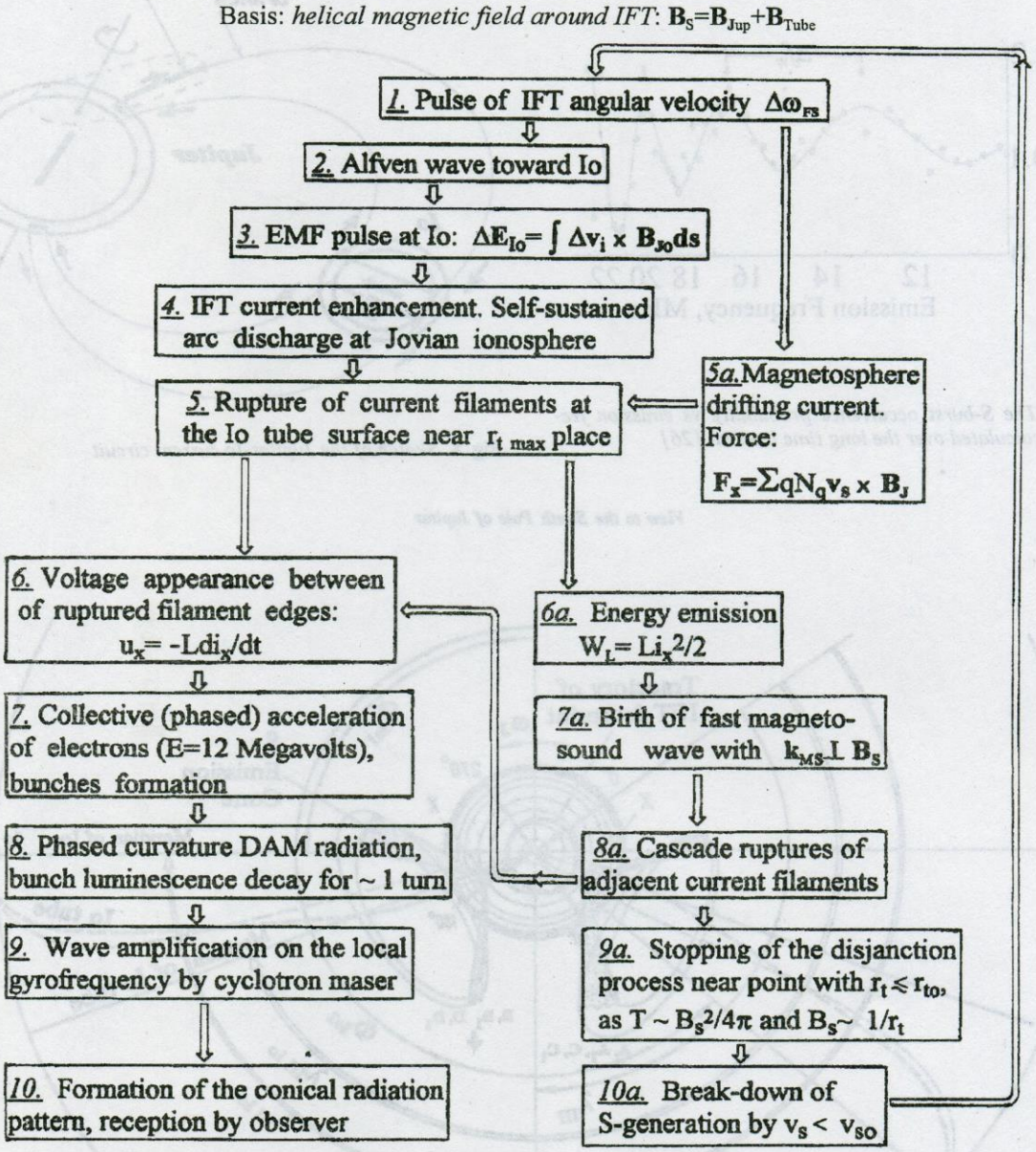

Fig. 10. *The scheme of the S-emission operation algorithm*

i. e. the vector sum of Jupiter's own magnetic field $\mathbf{B}_J$ and tube current magnetic field $\mathbf{B}_T$. The explosion energy $W_L = Li_x^2/2$ released at the disruption point can excite a fast magneto-sound wave, propagating at the Alfven velocity normally to the helical magnetic field $\mathbf{B}_S$ around tube, and causing the ruptures of adjacent current filaments. The relativistic electron bunches moving along the magnetic field $\mathbf{B}_S$ produce linearly polarized coherent relativistic curvature radiation (or the magneto-drift radiation) registered by an observer as the S-emission.

The directivity of the relativistic radiation is a the pencil beam pattern directed along the bunch velocity vector $\mathbf{v}_e$. The rotation of the pencil beam defined by the motion of electron bunches along the helical field $\mathbf{B}_S$ and around IFT produces the well known hollow cone pattern of S-radiation (See Figs. 9 and 11). The asymmetry of cone walls appears because of the curvature of the IFT axis in the meridional plane [28,30,31].

In such a manner, a drifting S-burst is generated by a cascade process of disruption of adjacent current filaments. The burst duration can be interpreted in terms of diameter modulation of IFT along its axis, as shown in Fig. 11. The magnetic tension of filaments on the tube surface, $B_S^2/4\pi$, weakens at wider places, since $B_S \sim 1/r_S$ (r_S is the tube section radius). So, the stability of the surface filaments is decreased on the "bulbs" and may result in a chain disjunction process. Therefore, S-emitters seem to be located as a rule at the widened zones of the tube (Fig. 11).

According to the just described scenario, if the triggering disruption of a current filament occurs somewhere below the bulb width maximum, the produced radiation is of small intensity and higher frequency (thin upper frequency end). The examples of such bursts are shown in Fig. 5.

This scenario reflects an idealized picture of currents and magnetic fields in the generation zone. Two characteristic stages of the IFT excitation can be identified in observational data. At the first one the current filaments can break up, but the field topology is not strongly distorted yet. This corresponds to quasi-regularly spaced ("rain like") simple and linear in f-t plane spectra of S-birsts (see Fig. 1.). At the second stage of the tube excitation we have a drastically disturbed field structure that leads to very complicated patterns of individual S-bursts, like the spectral shapes shown in Fig. 2, Fig. 3, or Fig. 4. Thus we interpret the complexity of S-burst patterns as a consequence of the complicated topological structures of the magnetic field lines and currents in the highly excited radiating area of IFT.

5. Large Scale Dynamics of IFT

According to our assumption [31, 32] the bandwidth of S-burst bands and the gap between adjacent ones correspond to the scale of bulbs on the IFT surface or, in other words, to a size of periodic modulation of the IFT diameter. Taking into consideration the mentioned above drift of the spectral bands, we encounter the phenomenon of moving bulbs along the IFT towards the planet's surface. Another interesting feature of the large scale dynamics of the IFT is the change of characteristic size of the bulbs (and corresponding bandwidth of S-emission bands) as they move along the tube. So, the phenomenon of frequency drift of the bands and change in their bandwidth can be interpreted in terms of the large scale dynamics of IFT.

Following the hypothesis of the S-generation at local electron gyrofrequency, we can estimate, from the spectral data available (as is shown in Fig. 6), the characteristic size M_x of the widening zone and its velocity $\mathbf{v}_b$ at the moment of observation. By sampling the experimental drift rate and using the empiric formula [28] for the altitude h of the S-radiation place in the Io tube:

$$h \approx 1.46 \cdot 10^6 f^{-1.44} \text{ (km)},$$

where f is in MHz, and relating the altitude of the S-radiation place h to the emission frequency in the IFT, one can estimate the bulb velocity towards the planet as

$$v_b = dh/dt = (dh/df)(df/dt)_{sb}.$$

For the value of the drift $(df/dt)_{sb} \approx 1.4$ kHz/s we have $v_b \approx 3$ km/s.

If the bandwidth of an S-burst corresponds to the scale of a bulb on the surface of IFT along its axis, the estimate the characteristic size M_x of the widening zone at the moment of observation is given by [31]:

$$M_x \approx 2.1 \times 10^6 f^{-2.44} \, \Delta f \text{ (km)}.$$

For example, the evolution of the large scale geometry of IFT during the S-burst storm of the 1st of February, 1994, is shown in Fig. 12. As one can see, a large bulb by $M_x \approx 5000$ km moves to the planet's surface with an average velocity v_b about 3 km/s. The bulb corresponds to the bandwidth of S-emission about 4 MHz.

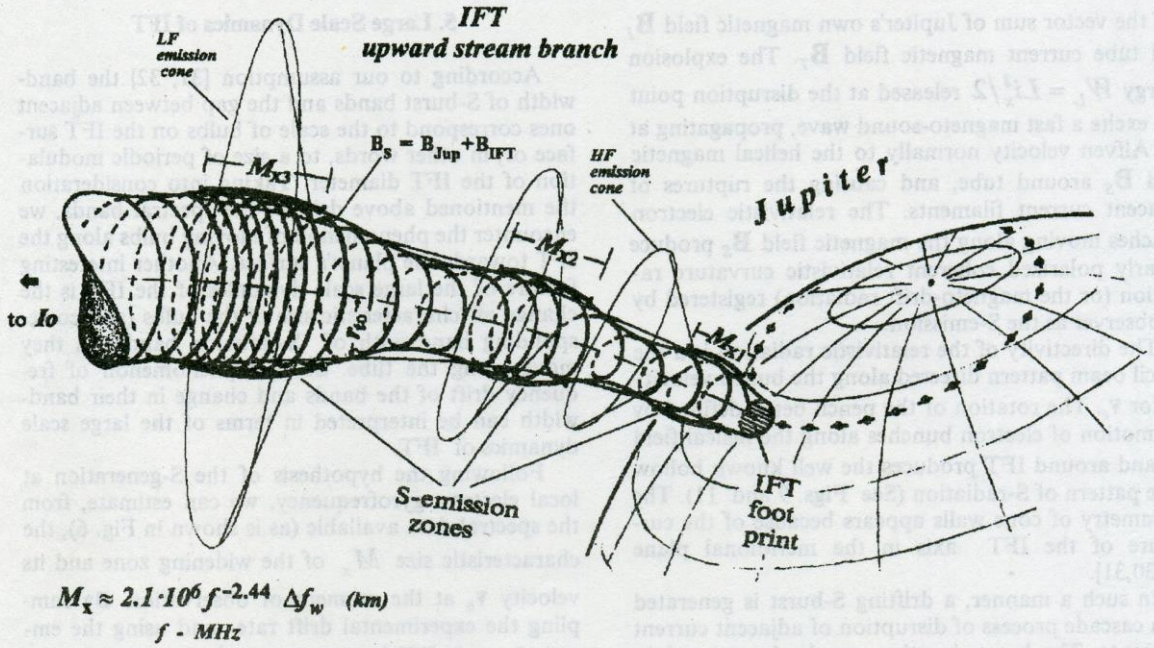

Fig. 11. *Scheme of IFT S-emission interval*

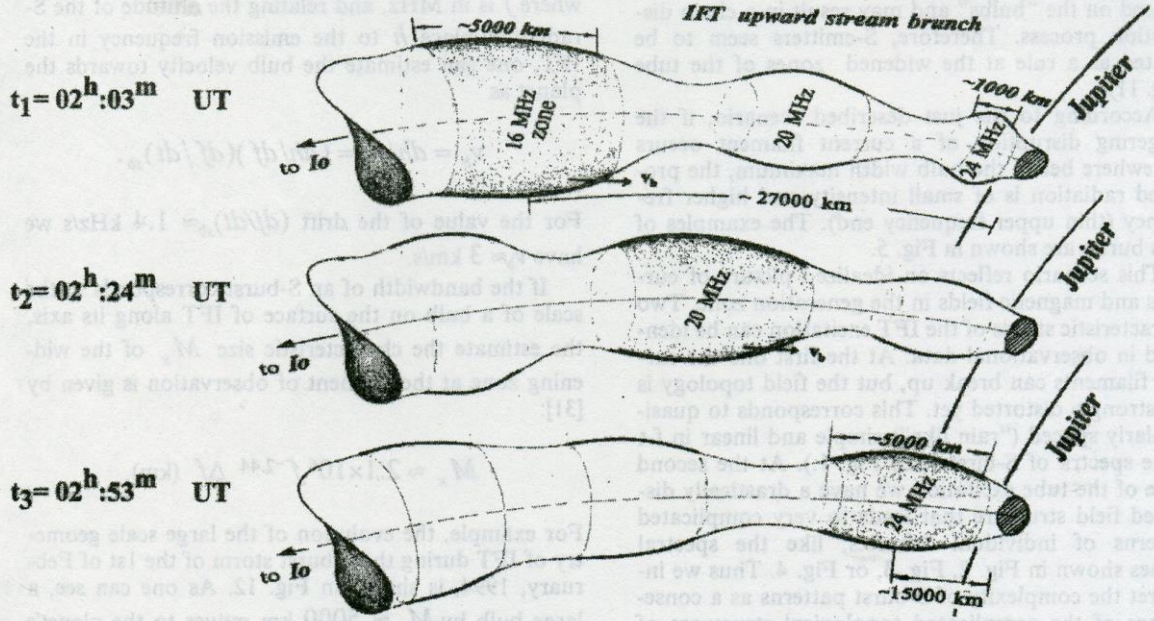

Fig. 12. *An evolution of large scale geometry of the Io tube during an S-burst storm (01 Feb.1994, Io-B)*

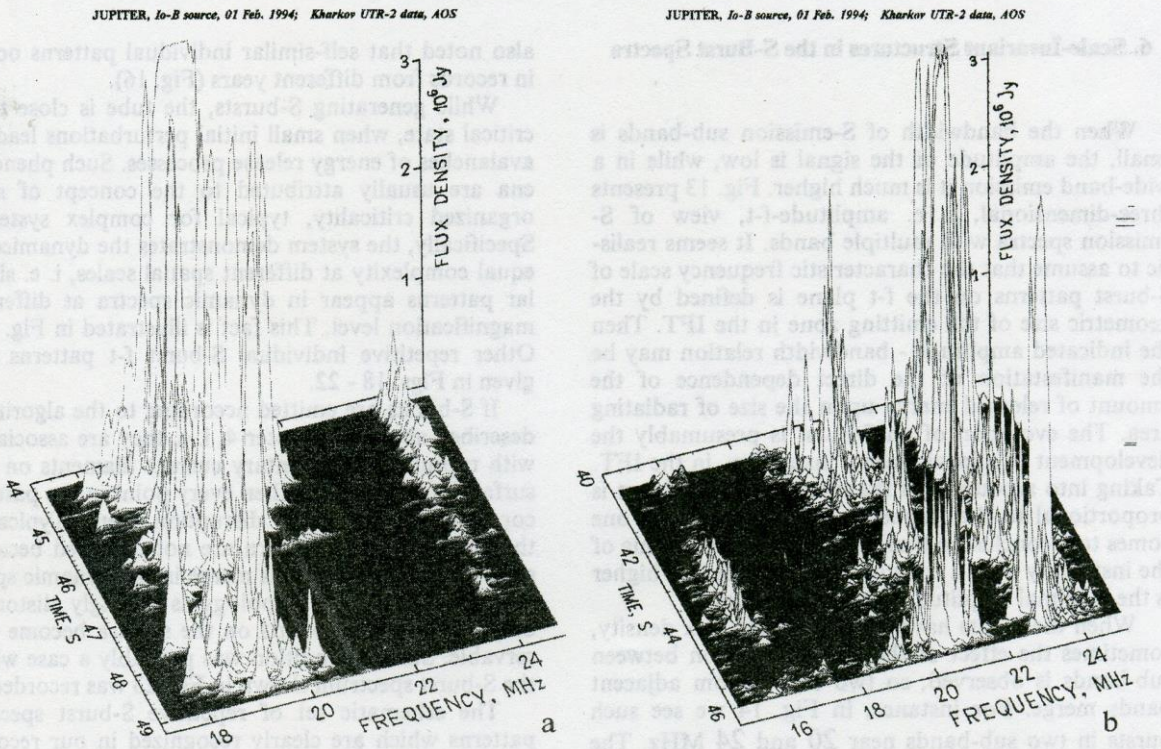

Fig. 13. *Three dimensional, amplitude-f-t S-burst spectral images with two subbands:* ***a)*** *narrow band, weak emission site is at upper frequencies, and wide band, strong emission takes place at low frequencies,* ***b)*** *after 14 minutes from the situation on the spectrum shown in previous picture, we observe the three-subbands spectral pattern with mutual exchange of places of the weak and strong bursts: narrow band, weak emission site is at lower frequencies, and wide band strong emission has moved to high frequencies*

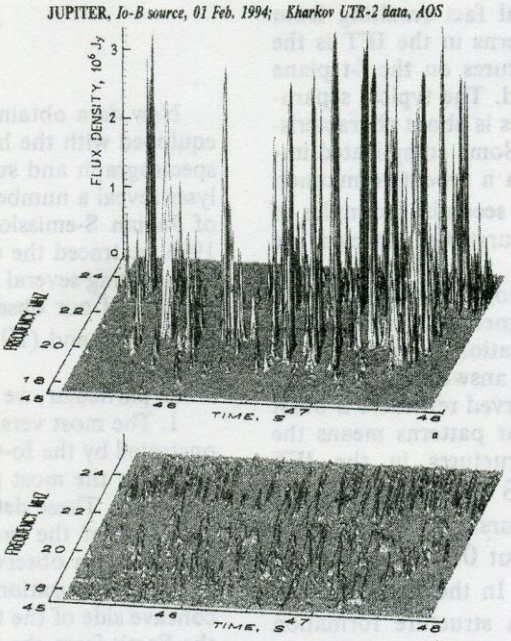

Fig. 14. *The S-emission pattern overlapping over the silence zone (band around 22 MHz) by individual, very powerful bursts, located at upper and lower frequency subbands:*
a) *an example of dynamic spectra of the powerful S-bursts in the three dimensional, amplitude-f-t space,*
b) *the same spectra with restricted burst amplitudes that show the foot parts of the powerfull pulses*

6. Scale-Invariant Structures in the S-Burst Spectra

When the bandwidth of S-emission sub-bands is small, the amplitude of the signal is low, while in a wide-band emission it is much higher. Fig. 13 presents three-dimensional, i. e. amplitude-f-t, view of S-emission spectra with multiple bands. It seems realistic to assume that the characteristic frequency scale of S-burst patterns on the f-t plane is defined by the geometric size of the emitting zone in the IFT. Then the indicated amplitude - bandwidth relation may be the manifestation of the direct dependence of the amount of released energy upon the size of radiating area. The evolution of an S-burst is presumably the development of a local plasma instability in the IFT. Taking into account that the lifetime of an S-burst is proportional to the frequency band it occupies, one comes to a conclusion that the longer is the lifetime of the instability with a constant growth rate, the higher is the maximal amplitude the burst reaches.

When the bursts have extremely high flux density, sometimes the effect of the gap intersection between sub-bands is observed, so two bursts from adjacent bands merge. For instance, in Fig. 14 we see such bursts in two sub-bands near 20 and 24 MHz. The total bandwidth of the bursts reaches the value of 7 MHz. Probably, in this case we encounter the phenomenon of passing over the saddle point between emitting zones on the Io tube surface by the moving disruption process (Fig. 11).

An interesting observational fact resulting from the formation of spectral patterns in the IFT is the repetition of similar fine structures on the f-t plane with time during a short period. The typical separation between such fine structures is about characteristic lifetime of the image itself. Some complicated images on the f-t plane appear in a repetitive manner, from 2 to 10 times in about 3 seconds. Examples of such repetitive individual S-burst f-t patterns are given in Fig. 15.

Now, let us ask the question: what defines the characteristic lifetime of a magnetized plasma structure responsible for the generation of a particular type of an S-burst pattern? The answer can be conjectured from the analysis of observed repetitive S-burst images. The sequence of similar patterns means the formation of quasi-stable structures in the IFT plasma with typical lifetime $2\div3$ times larger than the duration of an individual S-burst. In other words, within the time interval of about 0.5 s two or three similar patterns can be found. In the next $10\div15$ s the conditions for the plasma structure formation may be reproduced again giving rise to a similar repetitive pattern. So, we presumably encounter the phenomenon of local quasi-regular pulsation of plasma and magnetic field parameters. It should be also noted that self-similar individual patterns occur in records from different years (Fig. 16).

While generating S-bursts, the tube is close to a critical state, when small initial perturbations lead to avalanches of energy release processes. Such phenomena are usually attributed to the concept of self-organized criticality, typical for complex systems. Specifically, the system demonstrates the dynamics of equal complexity at different spatial scales, i. e. similar patterns appear in dynamic spectra at different magnification level. This fact is illustrated in Fig. 17. Other repetitive individual S-burst f-t patterns are given in Figs. 18 - 22.

If S-bursts are emitted according to the algorithm described above in chapter 4, i. e. they are associated with ruptures of elementary current filaments on the surface of IFT [31,32], then every point in the pattern corresponds to a single disruption event. Typically, the dots in S-burst spectra are not observed because close adjacent disruptions merge in the dynamic spectra. When the tube topology is strongly distorted only, the brightest points on the spectra become observable. Such a condition was probably a case when the S-burst spectrum shown in Fig. 23 was recorded.

The schematic set of repetitive S-burst spectral patterns which are clearly recognized in our records on the frequency-time plane is given in Fig. 24. Each pattern from the set presented may appear at different amplitude-time-frequency scales, i. e. they do possess the property of scale invariance.

7. Conclusions

New data obtained with the high sensitivity array equipped with the high f-t resolution acousto-optical spectrograph and superfast digital multichannel analyser reveal a number of previously unknown features of Jovian S-emission. In the observations of 1994-1996 we traced the evolution of the fine spectral patterns during several S-burst storms. The distinguished features of our observations are the continuous wide frequency band (10 MHz) and long tracking time of the planet.

In particular, we have detected the following.

1. The most versatile S-burst f-t patterns are demonstrated by the Io-C source, whereas the Io-B source generates the most powerful and comparatively simple bursts. These details can be explained by different geometry of the radiation interval of the IFT with respect to an observer. The Io-C source corresponds to the configuration when the observer looks to the concave side of the tube, and Io-B radiation comes to the Earth from the convex side of the IFT. It should be also noted that well organized quasi-linear patterns occur comparatively seldom, and often the dynamic spectra consist of random-like patterns.

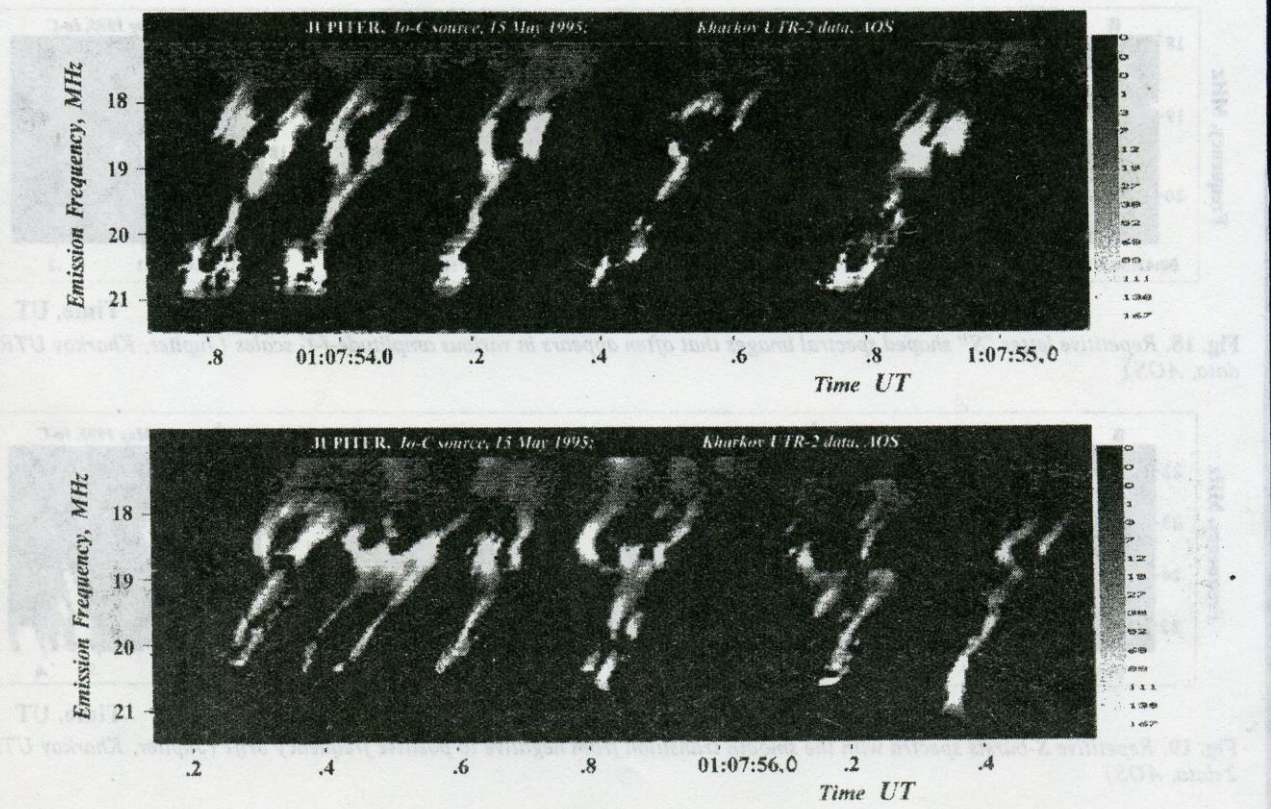

Fig. 15. *Repetitive, quasi periodic, complicated spectral images of individual S-bursts extracted from the direct spectral records*

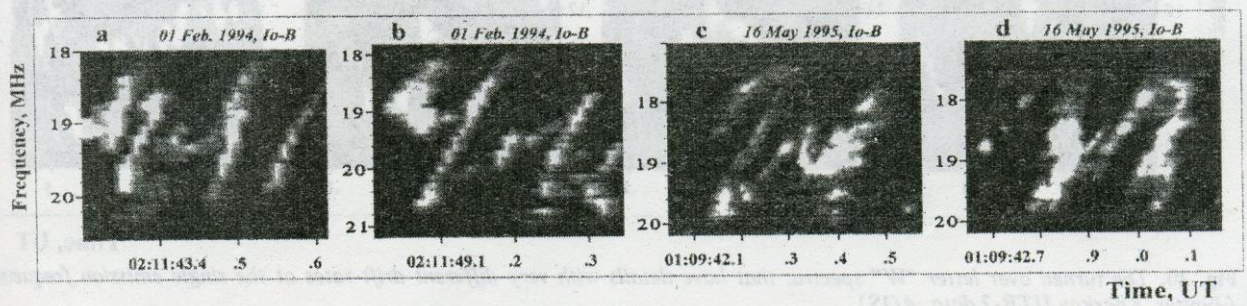

Fig. 16. *Complicated similar S-burst spectral images that appear in the records from various years (Jupiter, Kharkov UTR-2 data, AOS)*

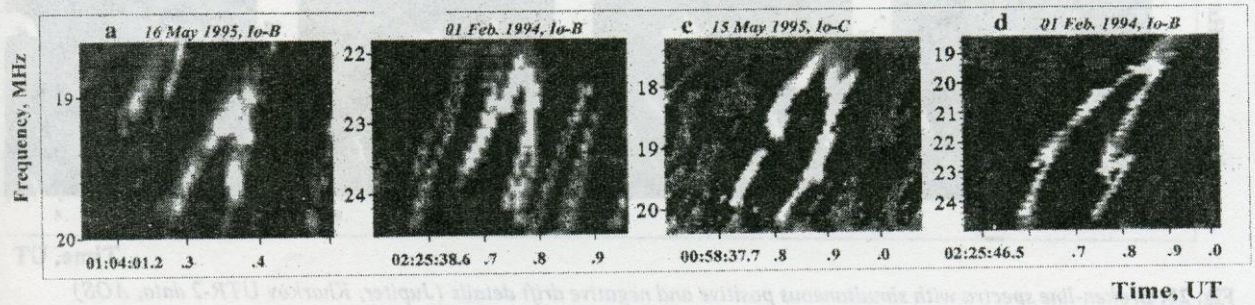

Fig. 17. *An apparent self-similarity of complicated S-burst patterns in different scales on f-t plane. The similarity factor is approximately equal to the bandwidth ratio of separate frequency subbands of S-bursts (see Fig.6a,b) (Jupiter, Kharkov UTR-2 data, AOS)*

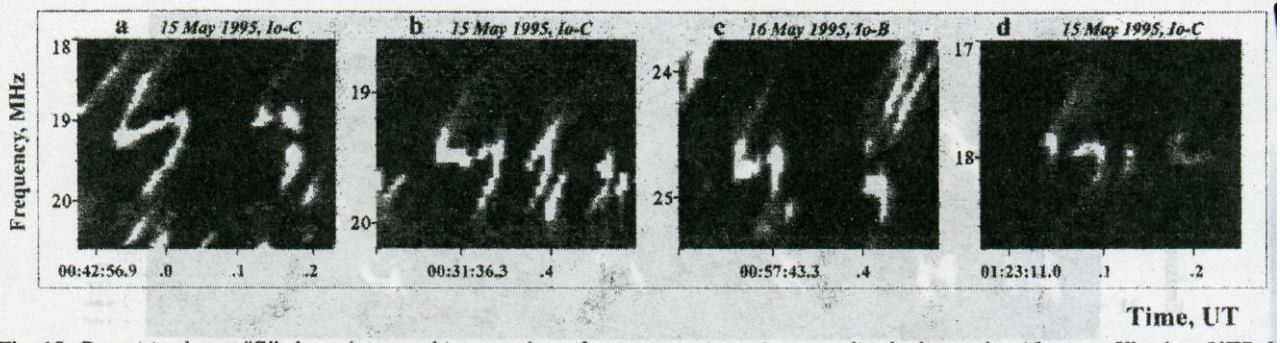

Fig. 18. *Repetitive letter "S" shaped spectral images that often appears in various amplitude-f-t- scales (Jupiter, Kharkov UTR-2 data, AOS)*

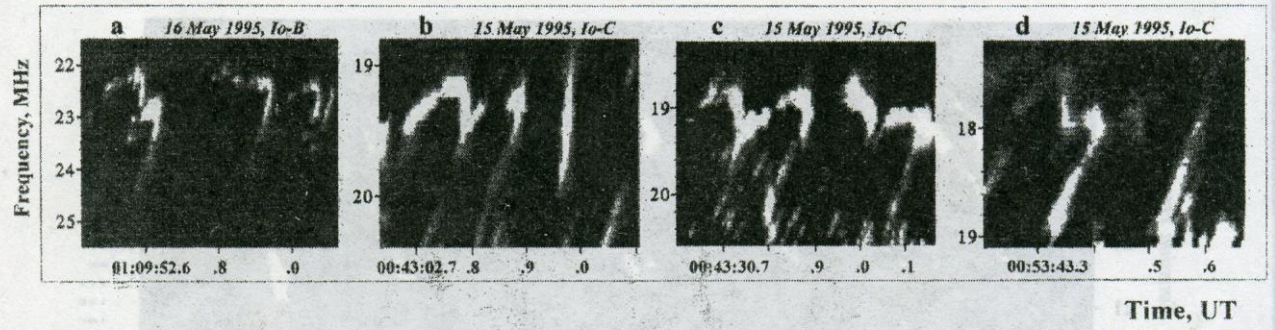

Fig. 19. *Repetitive S-bursts spectra with the smooth transition from negative to positive frequency drift (Jupiter, Kharkov UTR-2 data, AOS)*

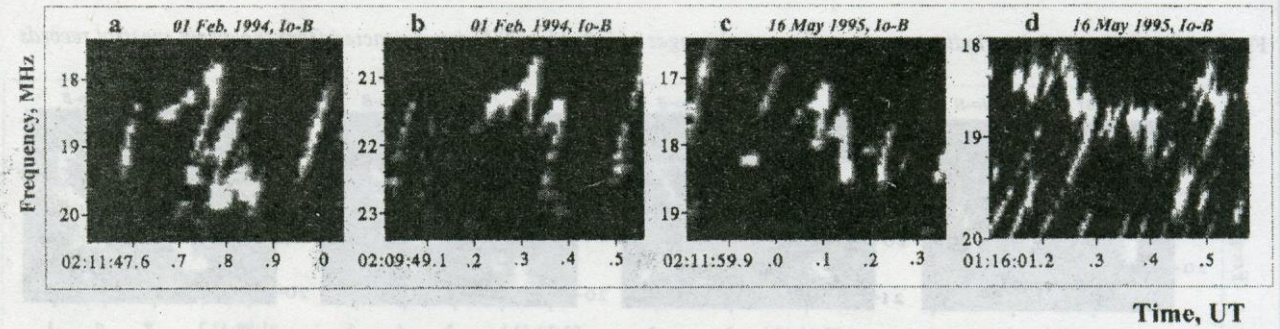

Fig. 20. *The turned over letter "W" spectra, that have details with very different drift rates at the single emission frequency (Jupiter, Kharkov UTR-2 data, AOS)*

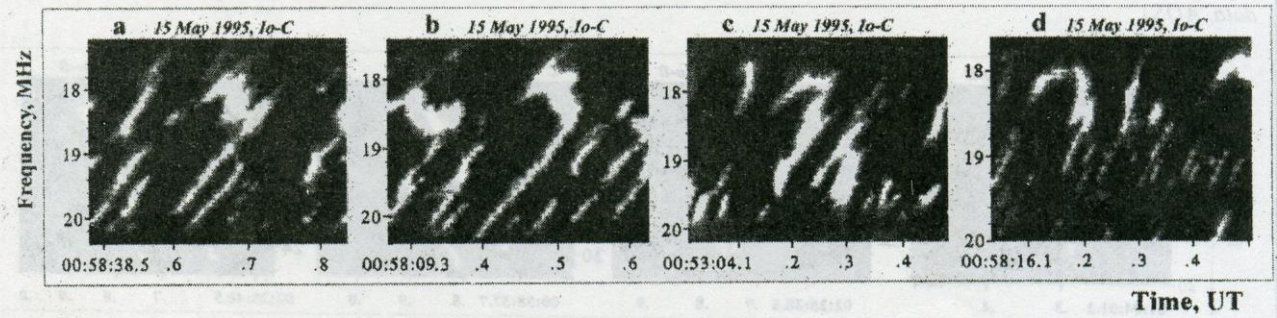

Fig. 21. *Broken-line spectra with simultaneous positive and negative drift details (Jupiter, Kharkov UTR-2 data, AOS)*

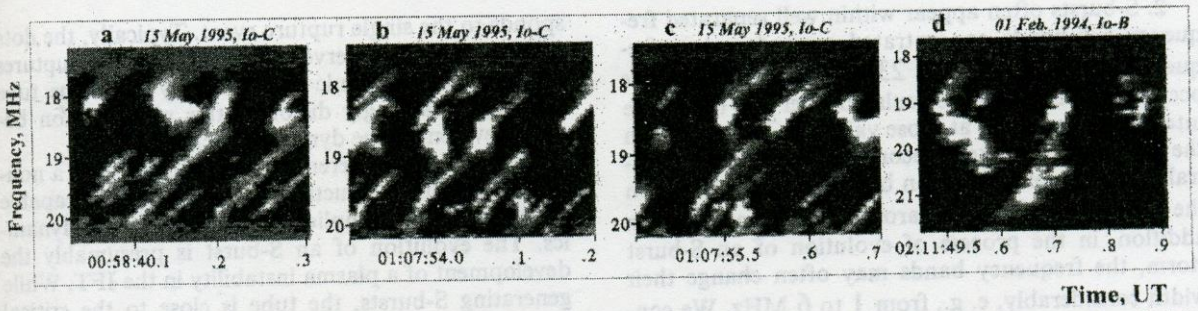

Fig. 22. *The S-bursts spectral patterns like letter "y". Individual details of the complicated spectra may have a positive drift in close vicinity of the negatively drifting parts. Self- similar "y"-shaped images may occurs about 10 times during of about 3 sec separated by quasi-equal intervals (Jupiter, Kharkov UTR-2 data, AOS)*

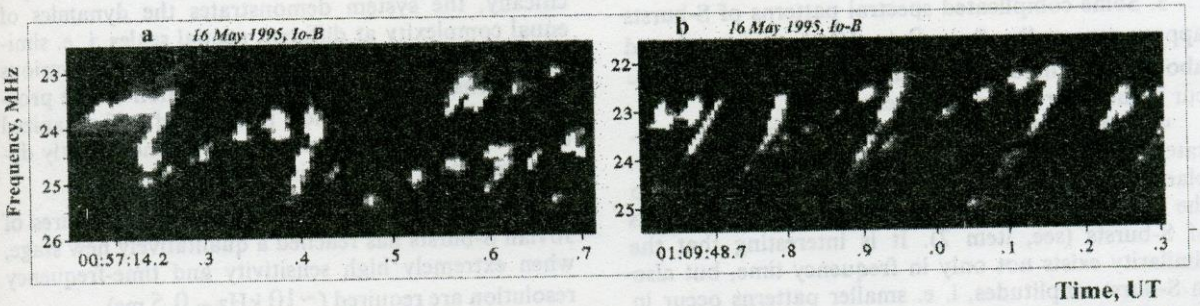

Fig. 23. *Dotted images of S-burst spectra: the distinct bright points on the spectrum become visible when the magnetic field topology and current circuits at the Io tube surface are strongly distorted (Jupiter, Kharkov UTR-2 data, AOS)*

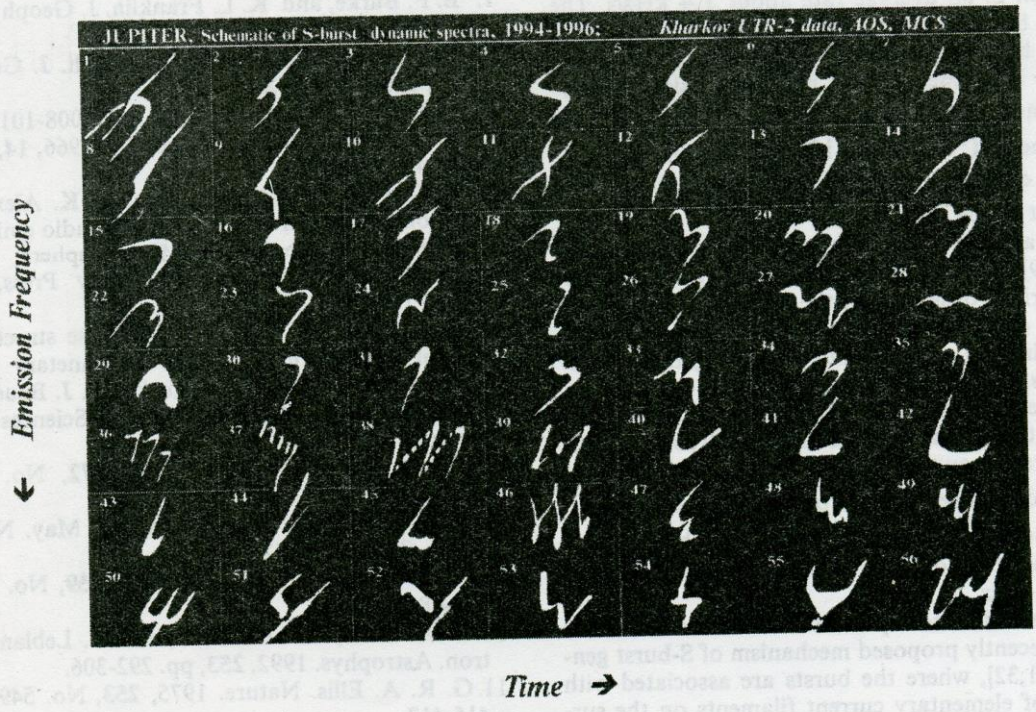

Fig. 24. *The set of schematic images of Jovian S-burst dynamic spectra. Similar S-burst patterns are clearly recognized in our records. The shapes shown have been repeatedly observed during observational campaigns in 1994-1996*

2. S-bursts often appear within well separated frequency sub-bands concentrated around certain frequencies of 13, 16.5, 20, 23.5, and 27 MHz . The occurrence probability calculated over the long time intervals has maxima at those values [26]. However, in the time scale from tens seconds to minutes, the central frequency of S-emission band may deviate within the range about 1.5 MHz around the mean values. In addition, in the process of evolution of an S-burst storm, the frequency bands may often change their width considerably, e. g., from 1 to 6 MHz. We conclude that this phenomenon may originate from large scale dynamics of the IFT, when the movement of the widening zones in IFT (bulbs) with simultaneous change in their characteristic size takes place.

3. Some complicated spectral patterns of S-bursts appear repeatedly, from 2 to 10 times in a period about 3 s. These self-similar individual patterns occur in the records from different years.

4. There is an apparent self-similarity of complicated S-burst patterns at different scales on the f-t plane. The similarity factor is approximately equal to the bandwidth ratio of separate frequency subbands of S-bursts (see, item 2). It is interesting that the similarity exists not only in frequency-time, but also in S-burst amplitudes, i. e. smaller patterns occur in narrow sub-bands and always have lower amplitudes.

5. Our observations present such new spectral details as slow positive frequency drift of sub-bands of S-emission at an average rate about 1.4 kHz/s. The drift can be interpreted as a result of slow motion of the IFT bulbs towards the planet surface. By sampling the experimental drift rate and using the empiric formula for the altitude h of the S-emission location in the IFT: $h \approx 1.46 \cdot 10^6 f^{-1.44}$ (km), where f in MHz, one can estimate the bulb velocity towards the planet as $v_b \approx 3$ km/s.

6. As a rule, traditionally expected and well interpreted [49] fine structure of S-burst with negative frequency drift is observed. At the same time, some parts of many complicated spectral patterns may have a positive drift, in close vicinity of the negatively drifting details.

7. The S-bursts with rather simple quasilinear shape on the f-t plane reveal intrinsic structure at the highest frequency-time resolution and sensitivity of the telescope. The spectral patterns resemble an $\int$ shape, when in the middle part of an $\int$ the fixed frequency duration of a burst is substantially greater than at its ends.

8. All the detected spectral features are consistent with the recently proposed mechanism of S-burst generation [31,32], where the bursts are associated with ruptures of elementary current filaments on the surface of the IFT. An additional confirmation for this viewpoint is the availability of dotted spectral patterns. Every point constituting the pattern corresponds to the single rupture event. Typically, the dots are not always observed because adjacent ruptures merge on the dynamic spectra. Only when the tube topology is strongly distorted this phenomenon becomes evident in the dynamic spectra.

9. The electric current system of the IFT is a nonlinear distributed structure and apparently is capable to demonstrate complicated spatiotemporal dynamics. The evolution of an S-burst is presumably the development of a plasma instability in the IFT. While generating S-bursts, the tube is close to the critical state, when small initial perturbations lead to avalanches of energy release processes. Such phenomena are usually attributed to the concept of self-organized criticality, typical of complex nonlinear systems. Specifically, the system demonstrates the dynamics of equal complexity at different spatial scales, i. e. similar spectral amplitude-f-t patterns appear at various resolutions. The proposed interpretation of the process of S-bursts generation in terms of self-organized criticality is generally consistent with the recently developed model of the radiation source.

10. The study of super fine spectral structures of Jovian S-bursts has reached a qualitatively new stage, when extremely high sensitivity and time-frequency resolution are required ($\sim$10 kHz – 0.5 ms).

References

1. B. F. Burke, and K. L. Franklin. J. Geophys. Res. 1955, **60**, pp. 213-217.
2. J. K. Alexander and M. D. Desch. J. Geophys. Res., 1984, **89**, pp. 2689-2697.
3. E. K. Bigg. Nature. 1964, **203**, pp. 1008-1010.
4. E. K. Bigg. Planet. and Space Sci. 1966, **14**, No. 8, pp. 741- 758.
5. T. D. Carr, M. D. Desch, and J. K. Alexander. Phenomenology of magnetospheric radio emissions, in Physics of the Jovian Magnetosphere, ed. by A. J. Dessler. Cambridge University Press, New York, 1983, pp. 226-284.
6. T. D. Carr, and F. Reyes. Subpulse structure of Jovian decametric S-bursts, in Planetary Radio Emission III, ed. by H. O. Rucker, S. J. Bauer, and M. L. Kaiser. Austrian Academy of Sciences Press, Vienna, 1992, p. 145.
7. M. D. Desch. Nature. 1978a, **272**, No. 5651, pp. 339-340.
8. M. D. Desch, R. S. Flagg, and J. May. Nature. 1978b, **272**, pp. 38-42.
9. G. A. Dulk. Astrophys. J. 1970, **159**, No. 2, pp. 671-684.
10. G. A. Dulk, A. Lecacheux, and Y. Leblanc. Astron. Astrophys. 1992, **253**, pp. 292-306.
11. G. R. A. Ellis. Nature. 1975, **253**, No. 5491, pp. 415-417.
12. G. R. A. Ellis. An Atlas of selected spectra of the Jupiter S-bursts, Univ. of Tasmania, Hobart, Tasmania, Australia, 1979, 197 p.

13. G. R. A. Ellis. Austral. J. Phys. 1982, **35**, pp. 165-175.
14. R. S. Flagg and M. D. Desch. Geophys. Res. 1980, **84**, pp. 4238-4244.
15. R. S. Flagg, W. B. Greenman, F. Reyes, T. D. Carr. A Catalog of High Resolution Jovian Decametric Radio Noise Burst Spectra, Dept. of Astronomy University of Florida, Gainesville, Florida 32611, vol. 1, 1991, 199 p.
16. Y. Leblanc, F. Genova, and J. de la Noe. Astron. Astrophys. 1980a, **86**, pp. 342-348.
17. Y. Leblanc, M. G. Aubier, C. Rosolen, F. Genova, and J. de la Noe. Astron. Astrophys. 1980b, **86**, pp. 349-354.
18. Y. Leblanc, and F. Genova. J. Geophys Res. 1981, **86**, No. 10, pp. 8564-8568.
19. J. J. Riihimaa. Astrophys. and Space Sci. 1977, **51**, No. 2, pp. 363-383.
20. J. J. Riihimaa. Earth, Moon and Planets. 1991, **53**, pp. 157-182.
21. J. J. Riihimaa. Wide-range high-resolution S-bursts spectra of Jupiter. Univ. of Oulu, Finland, 1992.
22. H. O. Rucker, and V. Mostetschnig. Interferometric observations at 16.7 and 22.2 MHz at the Observatory Lustbuehel, Graz, in Planetary Radio Emission II, ed. by H. O Rucker, S. J. Bauer, and B.M.Pedersen. Austrian Academy of Sciences Press, Vienna, 1988, pp. 87-93.
23. H. O. Rucker, V. Mostetschnig, H. P. Ladreiter, and G. K. F. Rabl. Spectrometric observations of Jupiter S-bursts at the observatory Lustbuhel, Graz, in Planetary Radio Emission III, ed. by H. O. Rucker, S. J. Bauer, and M. L. Kaiser. Austrian Academy of Sciences Press, Vienna, 1992, pp. 115-124.
24. J. W. Warwick, J. B. Pearce, A. C. Riddle, J. K. Alexander, M. D. Desch, M. L. Kaiser, J. R. Thieman, T. D. Carr, S. Gulkis, A. Boischot, C. C. Harvey, and B. M. Pedersen. Science. 1979a, **204**, No. 4396, pp. 995-998.
25. J. W. Warwick, J. B. Pearce, A. C. Riddle, J. K. Alexander, M. D. Desch, M. L. Kaiser, J. R. Thieman, T. D. Carr, S. Gulkis, A. Boischot, Y. Leblanc, B. M. Pedersen, and D. H. Staelin. Science. 1979b, **206**, p. 991.
26. B. P. Ryabov, A. V. Arkhipov, and V. A. Shevchenko. Astron. Vestnik. 1985, **19**, No. 4, pp. 296-318 (in Russian).
27. B. P. Ryabov. Astron.Vestnik. 1986, **20**, No. 1, pp. 20-34 (in Russian).
28. B. P. Ryabov, and N. N. Gerasimova. Sporadic radio emission of Jupiter at decameter wavelength. Kiev, Naukova Dumka, 1990a, 237 p. (in Russian).
29. B. P. Ryabov. Astron. Vestnik. 1990b, **24**, No. 2, pp. 103-118 (in Russian).
30. B. P. Ryabov. Astron. Vestnik. 1990c, **24**, No. 3, pp. 221-231 (in Russian).
31. B. P. Ryabov. Jovian S-emission: Decametric High sensitivity observations and model of radiation source, in Planetary Radio Emission III, ed. by H. O. Rucker, S. J. Bauer, and M. L. Kaiser. Austrian Academy of Sciences Press, Vienna, 1992, pp. 125-144.
32. B. P. Ryabov. J. Geophys. Res. 1994, **99**, No. E4, pp. 8441-8449.
33. M. L. Goldstein, C. K. Goertz. Physics of the Jovian magnetosphere. Ed. by A. J. Dressler. Cambrige, Cambr. Univ. Press, 1983, 317 p.
34. V. V. Zaitsev, E. Ya. Zlotnik, and V. E. Shaposhnikov. Pis'ma Astron. Zh., 1985, **11**, p. 208.
35. A. G. Boev, and M. Ya. Luk'yanov. Astron. Zh. 1991, **63**, pp. 853-862.
36. A. J. Willes, D. B. Melrose, and P. A. Robinson. Journ. Geophys. Res. 1994, **99**, No. A11, pp. 21203-21211.
37. B. P. Ryabov, V. B. Ryabov, H. O. Rucker, P. Zarka, M. Y. Boudjada. Some new features of Jupiter S-bursts from recent UTR-2 observations. International Workshop "The Solar Wind-Magnetosphere System 2", Graz, Austria, September 1995.
38. J. E. P. Connerny, M. H. Acuna, and N. F. Ness. J. Geophys. Res. 1981, **86**, No. A10, pp. 8370-8374.
39. J. E. P. Connerny. Doing more with Jupiter's magnetic field, in Planetary RadioEmission III, ed. by H. O Rucker, S. J. Bauer, and M. L. Kaiser. Austrian Academy of Sciences Press, Vienna, 1992, pp. 13-33.
40. J. E. P. Connerny. J. Geophys. Res. 1993, **98**, pp. 18659-18679.
41. M. Y. Boudjada, H. O. Rucker, H. P. Ladreiter, B. P. Ryabov. Astron. and Astrophys. 1995, **295**, pp. 782-794,
42. P. Zarka, B. P. Ryabov, M. Y. Boudjada, L. Denis. Recent observation of Jovian S-bursts, Magnetospheres of the Outer Planets. International Symp., Graz, Austria, August 8 - 12, 1994.
43. P. Zarka, B. P. Ryabov, V. B. Ryabov, et. al., Jovian decameter radio bursts from the vicinity of Io's flux tube. EGS Symposium PS-5.01: "Planetary Magnetospheres and Ionospheres", The Hague, Netherlands, May 1996.
44. P. Zarka, B. P. Ryabov, V. B. Ryabov, and H. O. Rucker. Ground based ultra-high sensitivity observations of planetary radio bursts at decameter wavelengths. Invited paper at EGS Symposium ST15/PS7, "Solar System Radiophysics and Related Topics", The Hague, Netherlands, May 1996.
45. S. Ya. Braude, A. V. Megn, B. P. Ryabov, N. K. Sharykin and I. N. Zhouck. Astrophys. and Space Sci. 1978, **54**, No. 1, pp. 3-36.
46. J. L. Green. Radio Science. 1984, **19**, No. 2, pp. 556-570.
47. P. Zarka. Beaming of planetary radio emissions, in Planetary Radio Emissions II, ed. by Rucker

S.J. Bauer, and B.M. Pedersen. Austrian Academy of Sciences Press, Vienna, 1988, pp. 327-342.
48. A. J. Dessler, and T. W. Hill. Astrophys. J. 1979, **227**, No. 2, pp. 664-675.
49. P. Zarka, T. Farges, B. P. Ryabov, M. Abada-Simon. J. Geophys. Res. Letters. 1996, **23**, No. 2, pp. 125-128,

ДЕКАМЕТРОВОЕ РАДИОИЗЛУЧЕНИЕ ЮПИТЕРА: Регулярные переменные явления и масштабные инварианты в динамических спектрах S-всплесков

Б. П. Рябов, Ф. Зарка, Х. О. Рукер, В. Б. Рябов, М. Боуджада

В новых радионаблюдениях Юпитера 1994-1996 гг. использовалась большая декаметровая антенна УТР-2 совместно с новой спектральной аппаратурой, состоящей из акусто-оптического спектрографа (АОС) высокого частотно-временного разрешения и быстродействующего многоканального спектрографа (МКС). В результате получено значительное количество новых динамических спектров S-всплесков тонкой структуры с минимальным потоком ~10 Ян в сплошном частотном диапазоне от 10 до 30 МГц. Как правило, S-всплески имеют общую тенденцию к отрицательному частотному дрейфу, но отдельные детали сложных спектров имеют положительный дрейф. Большинство изображений спектров отдельных всплесков имеют весьма сложную структуру, а хорошо известные линейно дрейфующие всплески составляют меньшинство в общем объеме данных. Приводится набор из 56 спектральных изображений индивидуальных S-всплесков, которые повторялись в указанный период наблюдений. Некоторые динамические спектры сложной формы показывают характерные черты самоподобных изображений с различным масштабом на частотно-временной плоскости. Другие типы всплесков появляются от 2-х до 10-ти раз подряд, повторяя самоподобную форму спектра в течение 3-х секунд. Одинаковые изображения встречаются на спектрограммах различных лет. Длинные временные последовательности S-всплесков концентрируются внутри спектральных полос, которые медленно дрейфуют по частоте (~1,4 кГц/с) и разделены интервалом ~3,5 МГц.

На основе полученных наблюдательных данных предложены алгоритм работы источника S-всплесков и схематическая картина движения крупномасштабных неоднородностей на излучающем интервале трубки Ио. Большинство обнаруженных свойств динамических спектров совместимо с предложенной нами ранее моделью источника S-излучения, в которой всплески обусловлены разрывами элементарных токовых нитей на поверхности трубки Ио.

ДЕКАМЕТРОВЕ РАДІОВИПРОМІНЮВАННЯ ЮПІТЕРА: Регулярні змінні явища та масштабні інваріанти в динамічних спектрах S-спалахів

Б. П. Рябов, Ф. Зарка, Х. О. Рукер, В. Б. Рябов, М. Боуджада

В нових радіоспостереженнях Юпітера 1994-1996 рр. використовувалась велика декаметрова антена УТР-2 разом з новою спектральною апаратурою, яка складається з акусто-оптичного спектрографа (АОС) високої частотно-часової роздільної здатності та швидкодіючого багатоканального спектрографа (БКС). Одержано значну кількість нових динамічних спектрів S-спалахів тонкої структури с мінімальним потоком ~10 Ян в суцільному частотному діапазоні від 10 до 30 МГц. Як правило, S-сплескам притаманна тенденція негативного частотного дрейфу, проте окремі деталі складних спектрів мають позитивний дрейф. Більшість зображень спектрів окремих сплесків мають досить складну структуру, а добре відомі лінійно дрейфуючі сплески становлять меншість в загальному обсязі даних. Приводиться набір з 56 спектральних зображень індивідуальних S-сплесків, котрі повторювалися в цей період спостережень. Деякі динамічні спектри сплесків складної форми мають характерні риси самоподібних зображень з різним масштабом на частотно-часовій площині. Інші типи сплесків з'являються від 2-х до 10-ти разів поспіль, повторюючи самоподібну форму спектра протягом 3-х секунд. Однакові зображення бувають на спектрограммах, одержаних в різні роки. Довгі часові послідовності S-сплесків зосереджуються всередині спектральних смуг, що поволі дрейфують по частоті (~1,4 кГц/с), и розмежовані інтервалом ~3,5 МГц.

На основі одержаних експериментальних даних запропоновано алгоритм роботи джерела S-сплесків та схематичну карту руху крупномасштабних неоднорідностей на інтервалі випромінювання трубки Іо. Більшість виявлених властивостей динамічних спектрів узгоджується з запропонованою нами раніше моделлю джерела S-випромінювання, в якій сплески обумовлені розривами елементарних токових волокон на поверхні трубки Іо.